View Article Online / Journal Homepage / Table of Contents for this issue

Chem Soc Rev

Published on 28 August 2009. Downloaded by Universitat Erlangen Nurnberg on 29/03/2016 08:56:33.

This article was published as part of the

2009 Green Fluorescent Protein issue

Reviewing the latest developments in the science of green fluorescent protein

Guest Editors Dr Sophie Jackson and Professor Jeremy Sanders

All authors contributed to this issue in honour of the 2008 Nobel Prize winners in Chemistry, Professors Osamu Shimomura, Martin Chalfie and Roger Y. Tsien

Please take a look at the issue 10 table of contents to access the other reviews

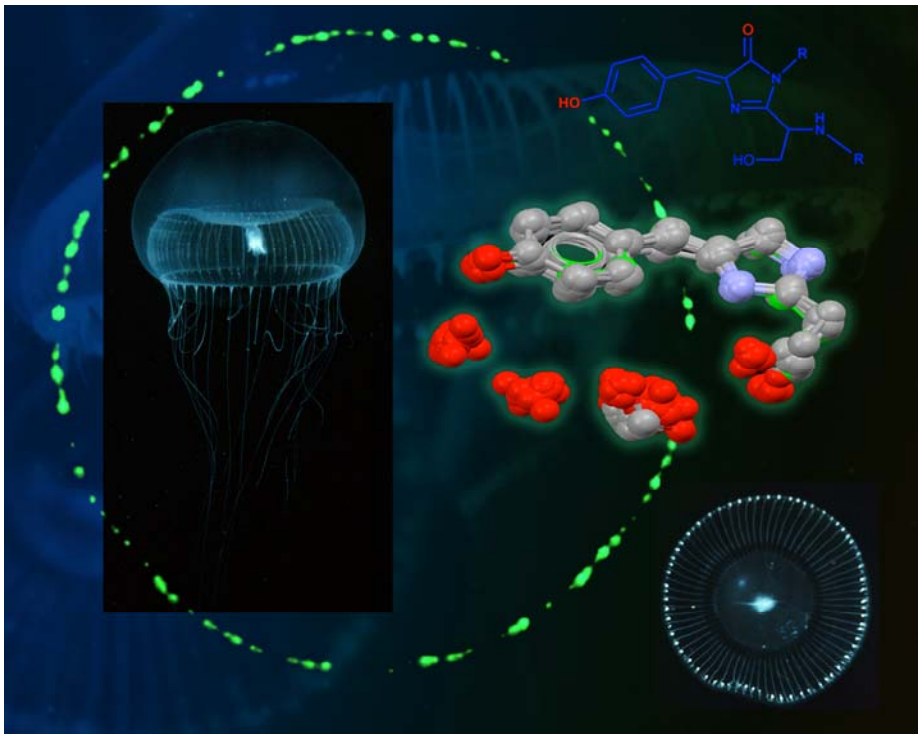

Photoreactions and dynamics of the green fluorescent protein†‡

Jasper J. van Thor*

Received 16th April 2009
First published as an Advance Article on the web 28th August 2009
DOI: 10.1039/b820275n

Published on 28 August 2009. Downloaded by Universitat Erlangen Nurnberg on 29/03/2016 08:56:33.

The wild type green fluorescent protein (GFP) from *Aequorea victoria* has been extensively investigated with a strong focus on the photochemistry and structural dynamics that are linked with its diverse activities. GFP combines a number of remarkable, and some unique, features that are still intensely researched both experimentally and theoretically. The protein environment effectively inhibits deactivation pathways that are dominant in the isolated chromophore and is therefore responsible for the bright fluorescence. Its *p*-hydroxybenzylidene-imidazolidinone chromophore acts as a photoacid, and optical excitation triggers ultrafast proton transfer reactions in the active site. The microscopic details of the proton transfer mechanism through a hydrogen bonding network are discussed in this *critical review*. This property of the wild type GFP has provided the opportunity to characterise the role of the specific protein environment in the proton transfer reactions in comparison to photoacid reactions in the condensed phase. In addition, GFP displays a photochromic side reaction that is uniquely caused by electron transfer from a buried anionic glutamic acid to the optically excited chromophore. This phototransformation property has also been exploited in high resolution fluorescence microscopy techniques. The discussion in this review is extended to include vibrational spectroscopy and structural dynamics (106 references).

1. Introduction

This contribution discusses the details of the photoreactions and dynamics of the wild type green fluorescent protein (GFP) from the jellyfish *Aequorea victoria* and is part of a themed issue in honour of the 2008 Nobel Prize winners in Chemistry, Professor Osamu Shimomura, Martin Chalfie and Roger Y. Tsien.

The discovery of GFP and the subsequent recombinant expression have been tremendously enabling for many fields of research. The spontaneous formation of the fluorescent molecule *in vivo* and the altered spectroscopic properties of genetically modified variants have resulted in the creation of many new tools in biology.[1] Following the discovery of the chemical nature of the auto-catalytically formed light absorbing *p*-hydroxybenzylidene-imidazolidinone chromophore[2,3] the X-ray crystallographic structure of GFP showed it to be buried in the central core of the folded protein[4,5] (Fig. 1). Based on this structural and chemical information, rational design of mutants with altered spectroscopic properties has been very successful. Presently there is a large diversity of available fluorescent proteins that are either modifications of *Aequorea victoria* GFP or native and modified fluorescent proteins from a number of other organisms. Modifications and differences of the chromophore structure itself and of the protein environment result in substantial spectral tuning and reactive properties that include electron and proton transfer as well as radical chemistry.[1,6–8] The wild type GFP, which is the subject of this review, remains the archetype for spectroscopic studies of the wider class of fluorescent proteins for several reasons. GFP is a highly fluorescent molecule, having a fluorescence quantum yield of 0.8.[1] In terms of absolute fluorescence quantum yield, the wild type GFP is still the brightest fluorescent protein available. The role of the protein matrix and the search for an answer to how it prevents deactivation mechanisms that are dominant in the isolated chromophore model compound

Division of Molecular Biosciences, South Kensington Campus, Imperial College London, London, UK SW7 2AZ.
E-mail: j.vanthor@imperial.ac.uk; Tel: +44-(0)20-75945071

† Part of a themed issue on the topic of green fluorescent protein (GFP) in honour of the 2008 Nobel Prize winners in Chemistry, Professors Osamu Shimomura, Martin Chalfie and Roger Y. Tsien.

‡ Electronic supplementary information (ESI) available: Links to view 3D visualisations of structures using FirstGlance. See DOI: 10.1039/b820275n

Jasper J. van Thor

Jasper van Thor uses time resolved spectroscopy and structural biology to investigate protein dynamics in light sensitive systems. He obtained his MSc and PhD degrees in Chemistry at the University of Amsterdam and subsequently moved to the Laboratory of Molecular Biophysics at Oxford University in 2000 to apply dynamical structural biology to problems of light activation. In 2002 he won a Royal Society University Research Fellowship to support the combined spectroscopic and structural work at Oxford. He took a position at the Division of Molecular Biosciences at Imperial College London in 2007 where he heads the ultrafast spectroscopy laboratory.

Published on 28 August 2009. Downloaded by Universitat Erlangen Nurnberg on 29/03/2016 08:56:33.

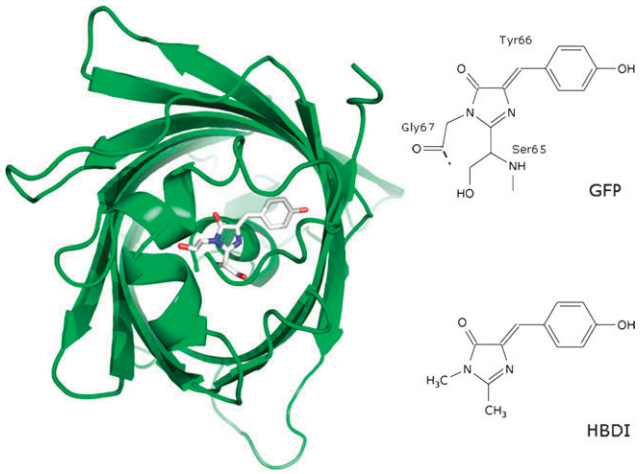

Fig. 1 The light absorbing *p*-hydroxybenzylidene-imidazolidinone chromophore of GFP is formed from internal cyclisation of Ser65, Tyr66 and Gly67, which becomes a conjugated photoacid structure.[2,3] The X-ray structure of GFP (PDB 1GFL)[4] and its mutant Ser65Thr (PDB 1EMA)[5] showed it to be a beta-barrel structure with the chromophore embedded in its core. A chromophore model compound 4-hydroxybenzylidene-1,2-dimethylimidazolinone (HBDI) is extensively used to investigate how the reactive and spectroscopic properties are tuned by the specific protein environment, and has aided vibrational mode assignments. The chromophore is shown in its neutral form, with the phenolic oxygen protonated, which corresponds to the dominant species "GFP_A", and absorbs maximally at λ_{max} = 398 nm.

4-hydroxybenzylidene-1,2-dimethylimidazolinone (HBDI)[9,10] is ongoing. The embedded *p*-hydroxybenzylidene-imidazolidinone chromophore makes highly specific contacts and hydrogen bonding interactions in the core of the beta-barrel structure (Fig. 1) which determines its excited state dynamics with very high efficacy. Another important reason for GFP to remain a strong focus for spectroscopic and theoretical investigations is the special fluorescence property of the wild type: the large Stokes shift of the fluorescence emission is a signature for its chromophore acting as a photoacid. One of the most important and illuminating discoveries regarding the photochemistry of GFP is that the photoacid chromophore triggers ultrafast excited state proton transfer (ESPT),[11] which will be further explored. Besides the dominant fluorescence pathway of GFP, an additional and low quantum yield light driven phototransformation process occurs, that has been exploited for high resolution fluorescence microscopy applications. This light driven process irreversibly transforms the blue light absorbing species (GFP_A; λ_{max} = 398 nm) into a green light absorbing species (GFP_R; λ_{max} = 483 nm) (Fig. 2). This photochromic reaction occurs with relatively low quantum efficiency, but complete accumulation of the photoproduct GFP_R is possible due to its irreversible nature and relatively inefficient competing photobleaching.[12] The underlying dynamics that respectively drive the fluorescence cycle and phototransformation, have provided a blueprint for approaching the diverse photochemical reactions that have been found in

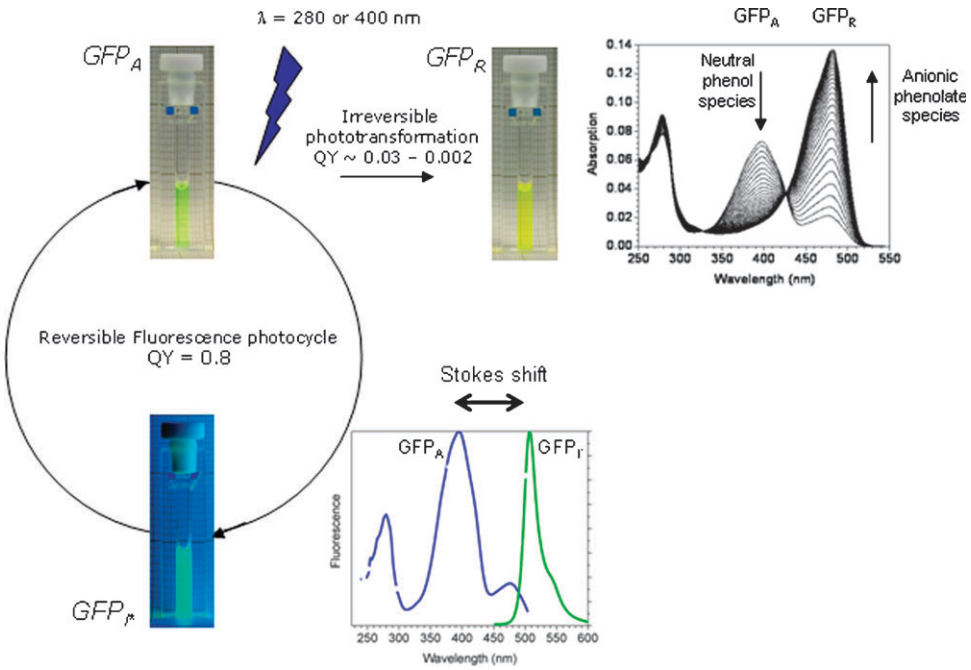

Fig. 2 Summary of spectroscopic properties of the fluorescence photocycle and the phototransformation reaction of wild type GFP. The chromophore of the dark resting state primarily exists in a neutral phenol form "GFP_A", absorbing maximally at 398 nm. In the dark, a minor population of an anionic species "GFP_B" absorbing maximally at 478 nm exists which has an anionic phenolate chromophore, for which the structural basis is well understood.[13–16] Upon visible excitation with UV (280 nm) or blue (400 nm) light, the dominant fluorescence pathway, which has a quantum yield of 0.8, leads to emission of green fluorescence at 508 nm from the excited anionic phenolate chromophore, designated the GFP_{I*} state (* denotes the excited state). The "Förster cycle" of GFP[11] links the size of Stokes shift as an energy term to the loss in proton affinity in the optically excited state, which triggers rapid deprotonation of the chromophore. A side-reaction, occurring with a quantum yield of 0.03 (280 nm excitation) to 0.002 (400 nm excitation), transforms the (green) dark resting state "GFP_A" into a (yellow) photoproduct "GFP_R". A time-series of absorption measurements indicates the complete transformation of the neutral form into the anionic form with continuous wave (cw) illumination at 280 nm.

 This journal is © The Royal Society of Chemistry 2009

Published on 28 August 2009. Downloaded by Universitat Erlangen Nurnberg on 29/03/2016 08:56:33.

other fluorescent proteins in recent years. The defining spectroscopic characteristics of the fluorescence and photo-transformation processes of GFP are depicted in Fig. 2.

The specific protein environment suppresses competing deactivation processes and tunes electronic transitions and branching between reactive pathways with remarkable specificity. The structural characterisation of the chromophore environment and its changes in the photoreactions have been addressed by X-ray structural and spectroscopic studies, a number of which are highlighted and discussed in detail below. X-Ray structural work on the wild type GFP, its photo-products, mutants and other related fluorescent proteins has accumulated systematic evidence with regard to the protein–chromophore interactions. Visible and vibrational spectroscopies have probed reactant, product and intermediate species in both the fluorescent and phototransformation pathways. GFP provides experimental access to microscopic details of protein function that have broad and significant impact in the life sciences.

2 Thermal proton transfer and equilibria

A central topic of interest concerns the non-equilibrium, light driven, proton transfer reactions of GFP. The current understanding of these rapid reactions is to an extent based on equilibrium proton transfer studies. The structural and spectroscopic characterisation of thermal proton transfer has led to many hypotheses for non-equilibrium transfer dynamics, which will be discussed in some detail in section 3. An overview of thermal proton transfer focuses on the available evidence for the wild type GFP.

The dominant spectroscopic species at neutral pH absorbs at 398 nm, which has been identified as the protonated neutral phenol species[9,17–19] (Fig. 1). The chemical nature of the chromophore was originally identified from mass spectrometry analysis of digested mature protein to be a phenolic chromophore consisting of an imidazolone ring that is formed by a post-translational modification of the tripeptide -Ser65-Tyr66-Gly67-.[9] pH titration of the chromopeptide identified protonation of the phenolic oxygen to be responsible for the blue-light absorbing species, and the deprotonated form for the green light absorbing species.[9] In the intact protein, a mixture of both protonated (“GFP_A”, λ_{max} = 398 nm) and deprotonated an anionic species (“GFP_B”, λ_{max} = 478 nm) species is present at neutral pH, albeit with a dominant population of the protonated form[20,21] (Fig. 2). When the X-ray structure of the wild type was solved, it was noted that the phenolic oxygen of the chromophore is in indirect hydrogen bonding contact with the carboxylate of the glutamate 222 side chain, which led to the proposal that electrostatic repulsion between the phenolic OH group and the ionic carboxylate in this network stabilises the protonated chromophore[4,13,16] (Fig. 3). From the X-ray crystallographic analysis, the protonation state of the glutamate carboxylate was inferred on the basis of the H-bonding interactions.[13,16] Direct proof was later obtained from FTIR difference spectroscopy, which showed that decarboxylation of the glutamate 222 side-chain does not lead to detectable absorption changes at a frequency of 1720 cm^{-1} which is characteristic of protonated carboxylate groups.[12,22] Therefore the glutamate 222 carboxylate group is predominantly anionic in the GFP_A ground state, which supports the model of indirect electrostatic repulsion between the chromophore and the glutamate 222 side chain as first proposed by Brejc *et al.*[13] With regard to the possible protonation state of the chromophore, the additional protonatable site, the heterocyclic ring nitrogen (Fig. 1), was addressed by X-ray crystallographic studies[23] and theoretical calculations initially at the intermediate neglect of differential overlap (INDO/S) semi empirical level[24,25] and multireference semi-empirical approaches,[26,27] with markedly different results. The X-ray crystallographic study, which addressed low (pH 4.6) and alkaline (pH 8.0) structures of the Ser65Thr mutant of GFP (pK_a = 6.0), concluded that the protonated species corresponds to protonation of the phenolic oxygen. In contrast, the early semi-empirical electronic structure calculations at the INDO level suggested that in the ground state the chromophore was in cationic form with both the heterocyclic ring nitrogen and the phenolic oxygen protonated[24,25] (Fig. 1). Excited state torsional profile calculations using multireference configuration interaction at the semi-empirical neglect of differential diatomic overlap (NDDO) level provided a direct explanation[26] of ‘blinking’ behaviour that was observed in single molecule spectroscopy,[28,29] by identification of a conversion between the fluorescent anionic and the dark zwitterionic forms as a possible deactivation route. The cationic species was assigned to the dark state, with identification of a non-adiabatic crossing for the excited state of the zwitterion.[26] On the basis of *ab initio* calculations, El Yazal *et al.* put forward that a mixture of the uncharged and zwitterionic species exists between pH 1.1 and pH 9.4 and that the chromophore becomes cationic below pH 1.1 and anionic above 9.4.[30] Experimental evidence that was in line with this proposal was obtained from resonance Raman spectroscopy of GFP of the free HBDI model compound and normal mode calculations.[17,31] Schellenberg *et al.* investigated the pH dependence of the visible and vibrational spectroscopy of the HBDI model compound in ethanol and reported maximum absorption for acidic, neutral and alkaline conditions at 400, 373 and 439 nm, respectively.[17] The results showed that the resonance Raman spectra of both GFP and neutral HBDI are dominated by a band at 1565 cm^{-1}, which was assigned to a mixed stretching mode having contributions of stretching of the imidazolinone C=N bond and the central C=C bond of the chromophore.[17] A Raman study that compared vibrational spectroscopy of a chromophore model compound ethyl 4-(4-hydroxyphenyl)methylidene-2-methyl-5-oxoimidazolacetate with spectroscopy of wild type and S65T mutant GFP arrived at a similar conclusion and argued that the neutral species is the predominant form in the wild type and the anionic form in mutant S65T.[31] The existence of mixed species over a large range from pH 7 to 12 follows directly from a model that assumes four dissociation constants which arise from the electrostatic interaction of two groups[14] (Fig. 3).

Spectral hole burning at cryogenic temperature identified two distinct anionic species: GFP_I and GFP_B, in addition to the GFP_A dominant neutral species.[15] The measurements determined the 0–0 transitions, which measure the energy

Published on 28 August 2009. Downloaded by Universitat Erlangen Nurnberg on 29/03/2016 08:56:33.

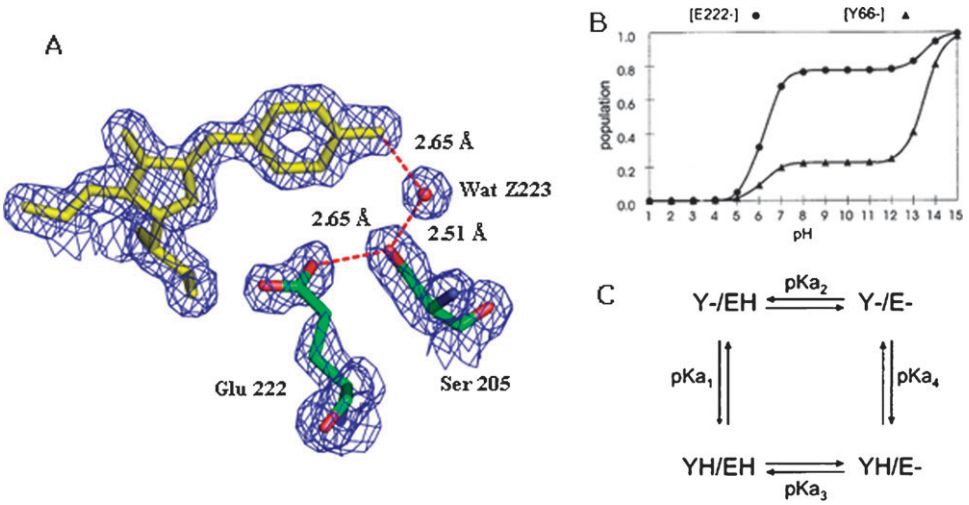

Fig. 3 Properties of thermal equilibrium proton transfer. (A) The X-ray crystallographic structure of wild type GFP showed the chromophore to be in indirect H-bonding contact with the carboxylate group of glutamate 222, *via* a crystallographic water molecule and the serine 205 side chain. Coordinates and 2Fo-Fc electron density map contoured at 1.6σ drawn from PDB 1W7S.[32] The discontinuous electron density of the Glu222 side chain indicates its partial disorder in the ground state, which is linked to heterogeneous kinetics for ESPT.[33] Electrostatic repulsion in the hydrogen bonding network was proposed to stabilise the protonated phenolate of the chromophore.[13] (B*) Electrostatic calculations generated the dissociation equilibria of the chromophore phenolic oxygen (Y66) and the Glu222 side chain (E222), which show a plateau between pH 7 and pH 12,[14] that reproduce experimental pH titrations.[18,19,34] (C*) A simple 4-state dissociation model for two interacting groups accounts for the titration behaviour that is observed.[14] * (B) and (C) are reproduced with permission from Scharnagl *et al.*[14]

separations of the pure electronic transitions from their vibrational ground states, at 495 nm and 477 nm for the two anionic species GFP_I and GFP_B, with the latter having greatest stability as observed at cryogenic temperatures. Additionally, at 1.6 K the ratio between the neutral and anionic forms, GFP_A and GFP_B, changes in favour of the anionic species, indicating it has slightly lower energy.[15] The high resolution hole burning experiments additionally identified possible pathways of interconversion. Burning into the GFP_A species at 1.6 K generated the GFP_I species, along the proposed pathway $GFP_A \rightarrow GFP_{A^*} \rightarrow GFP_{I^*} \rightarrow GFP_I$. Similarly, burning into GFP_B generates *via* a radiationless pathway the GFP_I species directly from GFP_{B^*}, and burning GFP_I generates GFP_A and GFP_B.[15] This work illuminated the complex spectral and dynamical characteristics of GFP at low and ambient temperatures and importantly identified two separate anionic species GFP_A and GFP_I.

3 Excited state proton transfer and intermediates in the fluorescence photocycle

Since the discovery of the photoacid nature of the HBDI chromophore in GFP,[11] many studies have focused on dissecting the structural details of the environmental response in the photoreactions. In 1996 Chattoraj *et al.* used fluorescence upconversion measurements to show that after excitation of the neutral species GFP_A, emission from the excited neutral species GFP_{A^*} detected at 460 nm, interconverts on picosecond timescale to a redshifted species emitting in the green at 508 nm.[11] In H_2O, GFP_{A^*} undergoes biphasic decay with time constants of 3.6 and 12 ps, whereas the redshifted emission of the deprotonated excited state GFP_{I^*} grows in with 2.2 and 8.1 ps time constants. Thus, the two decay phases of the excited neutral state match the two phases determined for the rise of the excited anionic species which demonstrates parallel interconversion with two time constants and no detectable intermediate in the excited state deprotonation reaction. Moreover, in D_2O, the time constants for decay of GFP_{A^*} and formation of GFP_{I^*} were shown to be much delayed at 22 and 116 ps and 8.2 and 46 ps, respectively. These experiments established the biphasic interconversion of a protonated and deprotonated excited state species and demonstrated its significant H/D kinetic isotope effect (KIE). Analysis of room temperature data indicated a KIE of 5 for the ESPT reaction.[11]

A KIE of this magnitude can either arise from multiple 'semi-classical' proton exchange reactions that takes into account only the altered zero point energy (ZPE) upon exchange and uses transition state theory (TST), or it could arise from extreme hydrogen tunneling.[35] To distinguish between these possibilities, the temperature dependence of the proton transfer rate and KIEs should be analysed over a large range of temperatures to allow a complete Arrhenius analysis which plots ln(KIE) *versus* $1/T$. In addition to a KIE that arises from a decreased ZPE of the deuterated species, the analysis seeks to distinguish an increase in the tunnelling barrier that results from the smaller de Broglie wavelength of the deuteron compared to the hydrogen (0.31 Å and 0.5 Å for H and D, respectively at 10 kJ mol^{-1} energy).[35] In the initial studies from Chattoraj *et al.* measurements of the GFP_{A^*} decay in H_2O were presented at the selected temperatures of 298, 120 and 85 K[11] that indicated substantially different kinetics of the proton transfer reaction but did not allow Arrhenius analysis. A recent study reported the time resolved fluorescence measurements of GFP over an extended temperature range both in H_2O and D_2O.[36] Using

 This journal is © The Royal Society of Chemistry 2009

Published on 28 August 2009. Downloaded by Universitat Erlangen Nurnberg on 29/03/2016 08:56:33.

time-correlated single photon counting (TCSPC) spectroscopy, measurements in H_2O were conducted in the temperature range of 13 to 293 K, and in D_2O from 84 to 293 K. The data analysis fitted rate constants for the forward ESPT reaction, in addition to a model dependent fit of the reverse reaction that includes explicit treatment of diffusion of the proton. The fitted rate of ESPT is least sensitive to the applied model and is the most suitable phase to assess for evidence for hydrogen tunnelling. Independent of the concave shape of the Arrhenius curve, in the low temperature region tunnelling should be expected to result in a temperature dependence of the H/D KIE because of a reduced de Broglie wavelength for the deuteron. Plots of the first derivative of the Arrhenius analysis (Fig. 4B) and the Arrhenius plot of the KIE, *i.e.* ln(KIE) *vs.* $1/T$ (Fig. 4C), do not indicate a substantial temperature dependence. Therefore, in the simplest analysis, experimental support for hydrogen tunnelling in the ESPT reaction from the currently available data is not yet conclusive, although theory that includes hydrogen tunnelling can explain concave Arrhenius curves. Beyond Arrhenius analysis, there have been several more involved approaches that take into account hydrogen tunnelling as the basis of data analysis. Using a model for vibrationally assisted hydrogen tunnelling from Trakhtenberg and Klochikhin,[37] Leiderman *et al.* analysed the temperature dependence of the ESPT and obtained a frequency of 210 cm^{-1} for the promoting vibration.[36] Within this model a good fit to the concave shape of the Arrhenius curve is obtained. Alternative treatments exist, that may also explain the non-Arrhenius behaviour. Specifically, a treatment of tunnelling reactions that is an extension of Kramers' rate reaction theory considered the temperature dependent behaviour from dissipative quantum tunnelling.[38] The temperature dependence of the dissipative processes leads to pronounced non-Arrhenius behaviour at low temperatures, that may also apply to GFP (Dan Huppert, personal communication). There does, however, not appear to be a consensus with regard to interpretation of non-Arrhenius behaviour and specifically convex and concave results, the latter being more common in biomolecular reactions. One interpretation includes the definition of the activation energy as equal to the average energy of molecules that react minus the average energy of all possible reactants. A concave shape of the Arrhenius plot, which indicates an increase of the activation energy with increasing temperature, may be explained using arguments taken from statistical thermodynamics. The energy averaged over all reacting systems increases more rapidly than that of the total population with increasing temperature because the unimolecular rate coefficient for a microcanonical ensemble, which denotes a closed system, increases as a function of energy.[39,40] An alternative interpretation that was also explored by Leiderman *et al.* considered two rate limiting processes that dominate in different temperature regimes and have very different activation energies. For the data in H_2O down to 13 K the fit provided values of two activation energies $Ea_1 = 6$ kJ mol^{-1} and $Ea_2 = 0.1$ kJ mol^{-1}.[36] These studies focused on the interpretation of the temperature dependence of the ESPT reaction primarily.

The magnitude of the KIE can be considered in the context of 'semi-classical' transition state theory that considers the zero point energy difference of the stretching mode along the reaction coordinate with the substituted isotope. As a model for the hydrogen bonded network in GFP (Fig. 3) values for the OH and OD stretching mode of phenol in water or deuterated water can be taken as 3524 and 2700 cm^{-1} respectively.[41] Taking the activation energy to be equal for both isotopes, the predicted single step KIE is obtained from:

$$\ln(\mathrm{KIE}) = \ln(k_H/k_D) = (\hbar\omega_H - \hbar\omega_D)/k_b T \qquad (1)$$

which at room temperature equals 2.35. The observed H/D KIE at room temperature is more than twice this value,[11] indicating a departure from a single step transfer in the semi-classical picture. However, the hydrogen bonding interaction between the phenolic oxygen of the chromophore and the carboxylate of glutamate 222 is indirect and includes an ordered water and a serine side chain (Fig. 3). Therefore multiple proton transfer reactions in this hydrogen bonded network are expected to lead to an increased KIE using the semi-classical treatment compared to a single proton transfer reaction.

Theoretical work has investigated the behaviour of the hydrogen bonded network in GFP. Molecular dynamics simulations that initiated proton transfer from the chromophore to the hydrogen bonded water observed femtosecond time-scale barrierless transfer from the water to serine 205 and following to glutamate 222.[42] Focusing on the initial proton transfer step, using CASSCF, CASPT2 and TDDFT level of theory, Vendrell *et al.* concluded that an electronic charge transfer state with σ* character intersects with the proton

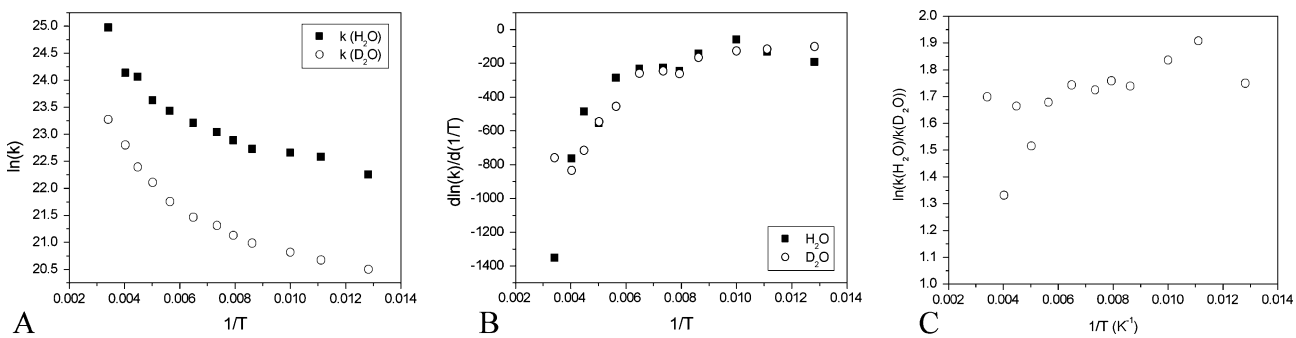

Fig. 4 (A) Arrhenius plot of the forward excited state proton transfer rate constants (ns^{-1}) in H_2O and D_2O. (B) First derivative of the Arrhenius plots of the ESPT reaction in H_2O and D_2O. (C) Arrhenius plot of the H/D KIE. Data taken with permission from Leiderman *et al.* (2008).[36]

Published on 28 August 2009. Downloaded by Universitat Erlangen Nurnberg on 29/03/2016 08:56:33.

transfer coordinate, that could provide a radiationless deactivation channel.[43] However, in a follow up study, potential energy profiles for the photoexcited state of the full quantum system were reported, that suggested that when the full proton transfer chain is considered, the intersection between σ* and π* configurations is no longer present due to stabilisation of the radiative species.[44] A systematic CASSCF and CASPT2 study of the potential energies of relevant configurations, in the absence of a specific model for the protein environment, suggested two possible mechanisms for the overall proton transfer to glutamate 222. In the energetically most favourable case the initial transfer would occur from the Ser205 proton, followed by transfer of the proton from the water molecule, and finally the proton of the chromophore. Alternatively, a synchronous, concerted motion process for the three protons would present a potential energy barrier of only 16.7 kJ mol^{-1} higher at the same level of theory.[44] The most recent study used quantum molecular dynamics of the proton wire between the phenolic proton, the hydrogen bonded water and simple models for serine 205 and glutamate 222 side chains.[45] The calculations at the multiconfiguration time-dependent Hartree (MCTDH) level predict two phases for the bond length and population changes upon promoting the ground state vibrational wave packet to the excited state. An initial ~20 fs phase is associated with the decay of the excited protonated chromophore, designated GFP_{A*}, followed by a slower ~200 fs for the remainder of the population. The calculations predict that all protons in the network behave close to synchronous. Simulations for the deuterated model indicate only a moderate KIE, that appears to be dominated by the raised ZPE of the deuteron only. Furthermore, a population of about 20% of the excited neutral state GFP_{A*} remained at the end of the simulations. Considering the experimental observation of the excited state pK_a being about 9 units (4200 cm^{-1}) below that of the ground state, as estimated from the Förster cycle,[11,14,46–48] and the very weak steady state emission at 460 nm from the neutral species of GFP, the excited state model used in this study may not have fully approached the real system with respect to charge relocation in the excited neutral state GFP_{A*}. The main observation of close to synchronous behaviour of protons in the wire, as well as the femtosecond time-scale of the expected population changes as opposed to the experimentally observed picosecond time-scale are important to evaluate in light of the experimental observations.

Within the 'semi-classical' picture of a synchronous triple proton transfer reaction, the KIE will increase due to accumulation of ZPE for all normal modes of the system. In the harmonic approximation that uses classical transition state theory the KIE equals:

$$\eta = \frac{\left(\frac{Q_{TS}}{Q_R}\right)^H}{\left(\frac{Q_{TS}}{Q_R}\right)^D} \qquad (2)$$

where Q_R and Q_{TS}, the partition functions for the reactant and the transition state, respectively, are:

$$Q_R = \prod_n q_n \qquad (3)$$

the product being over all n normal modes (q_n) of the system. In this treatment, the ZPE difference between the light and heavy isotopes increases with increasing number of contributing modes, resulting in an enlargement of the KIE. A synchronous situation has been analysed in the active site of carbonic anhydrase.[49] Rate kinetics theory however offers far more advanced treatment beyond approximations in semi-classical TST, that may be applied to GFP.[35,37,38,40,50]

The experimentally observed ESPT in H_2O is biphasic and proceeds with time constants ~3 and 10 ps with similar amplitude,[11,33,51] which is considerably slower than the simulated result. This may possibly indicate the existence of additional rate-limiting processes in the active site of GFP. Proton wires in GFP have been suggested to be more extended than the network including bound water, Ser205 and Glu222. It was pointed out on the basis of analysis of X-ray crystallographic coordinates that include refined waters that a proton wire may exist that links Glu222 near the chromophore with Glu5 on the protein surface.[52] When the room temperature fluorescence of the protonated species was followed for extended delay times, up to 15 ns, a non-exponential behaviour was observed. After correction of the curves for excited state decay using a single life time, an asymptotic dependence of $t^{-3/2}$ remains, that has been interpreted as proton diffusion in 3 dimensions reminiscent of ESPT reactions in solution (Fig. 5).[53–55]

Various models have sought to explain the asymptotic behaviour as it was noted that 3 dimensional diffusion within the protein is unlikely in view of the internal water content.[52] The possibility of reversible proton diffusion to the protein exterior was rejected when no concentration dependence of proton scavengers fluoride or acetate was observed.[53] On the basis of the $t^{-3/2}$ asymptotic behaviour of fluorescence, Agmon *et al.* have proposed a mechanism involving a switch mechanism, provided by the rotation of the Thr203 side chain, which eventually allows the proton to escape to the exterior solution.[52,54,56] An extension of these studies to incorporate the temperature dependence of the proposed proton transfer pathways led to remarkable results. Time-resolved fluorescence was fitted to a reversible model that explicitly included the

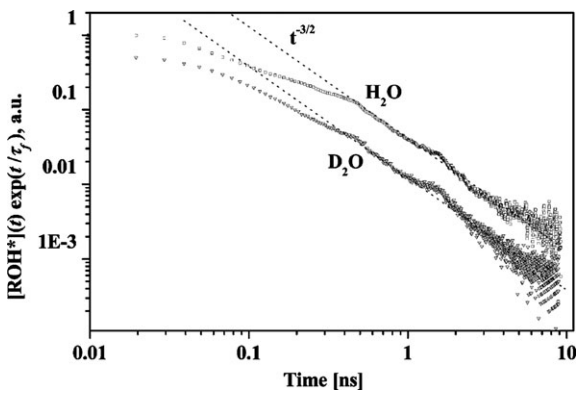

Fig. 5 The long-time fluorescence decay of GFP is non-exponential. The plot shows time resolved fluorescence intensity multiplied by the excited state decay, τ_{fl} = 3.2 ns, which reveals a remaining power law behaviour at long times, proportional to $t^{-3/2}$. Figure reproduced with permission from Leiderman *et al.* (2004).[53]

 This journal is © The Royal Society of Chemistry 2009

Published on 28 August 2009. Downloaded by Universitat Erlangen Nurnberg on 29/03/2016 08:56:33.

reverse proton transfer and diffusion processes. Focusing on the forward ESPT reaction, which is only moderately sensitive to the details of the applied model, it was observed that it had a maximum value at 230 K and in fact decreases at higher temperatures.[54] Also, except for the data included for room temperature, from separate fluorescence upconversion experiments, the rate constants reported by Leiderman *et al.* in 2006[54] are higher than those in the temperature dependence studies reported by the same authors recently.[36] The primary difference appears to be the inclusion of 30% glycerol in the samples in the 2006 study,[54] as opposed to use of distilled water.[36] In addition to a decrease of the ESPT rate above 230 K, the long-delay fluorescence behaviour showed a transition from asymptotic kinetics as $t^{-1/2}$ to $t^{-3/2}$, interpreted as a change from 1 dimensional to 3 dimensional diffusion.[52,54,56] The cause of the inverted kinetic effect at high temperatures may have different interpretations. It was suggested that a switch mechanism using the Thr203 side chain rotation was acting as a thermally activated gate, allowing 3 dimensional diffusion at high temperature.[54] Another proposal puts forward the possibility of increased disorder at high temperature that disrupts to some extent the synchronous behaviour of the proton chain (Noam Agmon; personal communication). A recent study explored the possibility that inhomogeneous proton transfer kinetics may result from a broad distribution of the distance between the donor and acceptor, particularly if tunnelling is considered.[57] In this model, inhomogeneous kinetics of both the forward, ultrafast ESPT reaction as well as the long-delay fluorescence behaviour are treated in an extension of the vibrationally assisted hydrogen tunnelling model, that fits available kinetic data well.[57] In terms of the molecular origin of the inhomogeneous kinetics of the forward ESPT reaction, this proposal is different from conclusions based on measurements of the heterogeneous structures of the glutamate 222 acceptor,[58] but with respect to the energetics it is similar in concept.

Time resolved vibrational spectroscopy has probed the molecular basis of the proton transfer mechanism, from which some important conclusions have emerged. Specifically, femtosecond optical excitation of the neutral species at 400 nm leads to absorption changes of an isolated band, in H_2O at 1725 cm^{-1},[33,59] which is a specific frequency for protonated carboxylic acid. In D_2O, a biphasic 15 and 49 ps growth was reported from single wavelength measurements at a lower frequency of 1706 cm^{-1}, on the basis of which an assignment to glutamate 222 was proposed.[59] The assignment was made on the basis of three observations:[33] (1) the isotope substitution effect of the mode, observed at a frequency of 1712 cm^{-1} in D_2O compared to 1725 cm^{-1} in H_2O supports the assignment to protonated glutamic acid. (2) The corresponding H/D KIE of the observed ESPT is about 5, which directly fits the KIE determined by fluorescence upconversion experiments[11] and (3) spectral and kinetic changes occur in a mutant Glu222Asp in which the proton acceptor is replaced with a functional aspartic acid 222 group. Specifically, ESPT was delayed relative to the wild type with 13 ps and 125 ps time constants in H_2O and D_2O respectively, and the COOH/D stretching mode of the carboxylate acceptor showed significantly reduced amplitude and downshifted frequency compared to the wild type.[33] However, analysis of long time delays indicates changes of the protonation state of the excited state proton acceptor; see below.

The details of the photocycle transitions and kinetics of GFP have been addressed by a number of ultrafast visible and vibrational spectroscopy investigations.[11,32,33,51,58–63] Following the discovery of the photoacid nature of GFP, it was postulated that after radiative decay the deprotonated chromophore, GFP_I, acts as a photocycle intermediate, before re-protonation occurs to reform the ground state GFP_A.[11] However, using time resolved visible absorption spectroscopy only the excited state species GFP_{A*} and GFP_{I*} could be observed.[61] Both fluorescence and visible transient absorption data are in agreement with respect to the biphasic ESPT process.[11,51,60,61] Fluorescence originating from the protonated excited state GFP_{A*} decays with similar lifetimes to the rise that is observed for the anionic excited state GFP_{I*}. Transient visible absorption spectroscopy observed an analogous result. With 400 nm excitation of GFP_A, an excited-state absorption band at 440 nm, and a broad stimulated emission band ranging from 450 to 550 nm assigned to GFP_{A*} is present at 400 fs. At longer time delays, a stimulated emission band with a maximum at 509 nm and a shoulder at 545 nm develops, which is a direct measure of the population of I*. Global fitting of these data is in agreement with the fluorescence measurements to support a biphasic ESPT reaction both in H_2O and D_2O, in addition to a KIE of 5.[51] The lifetime of the GFP_{I*} state is 3.0 ns, and no further intermediate is seen in experiments performed in H_2O before ground state GFP_A is recovered. A pump–dump–probe experiment that includes an additional pulse 20 ps after the 400 nm excitation targets the transient GFP_{I*} population which was resonantly 'dumped' at 540 nm to generate the corresponding ground state intermediate GFP_I that is normally hidden as the result of its low stability compared to GFP_{I*}. A red-shifted 'hot' state absorbing at 500 nm decays rapidly on the ps time-scale to form a secondary ground state intermediate which then finally becomes reprotonated to re-form GFP_A in 400 ps in H_2O. In D_2O, the re-protonation is much slower and occurs with an approximately 5 ns time-constant. This large KIE of about 12 also causes the transient accumulation of the GFP_I ground state, nanoseconds after excitation of GFP_A.[51] These results have provided the basis for interpretation of time resolved infrared experiments with GFP.[32,33,58,64]

Importantly, a reaction scheme with subsequent 10 and 75 ps (D_2O) phases where only one phase is associated with proton transfer must be rejected on the basis of single wavelength analysis at 1711 cm^{-1}, that shows biphasic induced absorption due to protonation of glutamate 222.[33,59] In addition, a successive reaction scheme for the 10 and 75 ps phases would also not be in agreement with transient visible absorption and fluorescence measurements that also support a biphasic ESPT reaction and deprotonation of the chromophore.[11,51,60,61] It has been established that the rise of fluorescence emission from the GFP_{I*} state at 509 nm is biphasic both in H_2O and in D_2O[11] and infrared measurements independently provide the same two time constants for the ESPT reaction.[32,58,59] ESPT therefore occurs during two parallel reactions that have approximately equal amplitude,

Published on 28 August 2009. Downloaded by Universitat Erlangen Nurnberg on 29/03/2016 08:56:33.

both in H_2O and D_2O. Whereas transient absorption and fluorescence spectroscopy did not resolve spectral differences between the two parallel ESPT reactions,[11,51] the difference mid-infrared spectra corresponding to the 10 ps ($GFP_{A1*} - GFP_A$) and 75 ps ($GFP_{A2*} - GFP_A$) components in D_2O did show distinct differences.[33] Assignment of 1456 cm^{-1} and 1441 cm^{-1} modes to ν_{sym} and 1564 cm^{-1} and 1570 cm^{-1} features to ν_{asym} of glutamate 222 in the 10 and 75 ps components, respectively, was possible from the analysis of the transient absorption data of an Glu222Asp mutant. In contrast to the wild type, measurements of Glu222Asp can be described with only one difference spectrum, with the ν_{sym} mode at 1435 cm^{-1} and the ν_{asym} mode at 1567 cm^{-1}, also correlating a large $\Delta\nu_{asym-sym}$ with slow ESPT kinetics. Therefore, both in the wild type and in the Glu222Asp mutant, a relationship is established between the configurational properties of the excited state proton acceptor and the overall rate of ESPT. The observation suggests that the conformation of the proton acceptor controls the kinetics, which would be consistent with recent predictions[44,65,66] that proton transfer from Ser205 to Glu222 initiates the ESPT reaction, but harder to reconcile with assumed initiation by proton transfer from the chromophore to the hydrogen-bonded water.[42] Such proposals that decouple the deprotonation of the chromophore and the protonation of Glu222 are not supported by fluorescence and infrared measurements that have established the parallel and biphasic deprotonation of the chromophore and protonation of Glu222, respectively. It was recently argued that the barrier for proton transfer from serine 205 to glutamate 222 that was calculated[44] may be high in view of the observed picosecond kinetics. Alternative models assume the functional operation of extended proton wires and switching mechanisms.[52,56]

Global fitting analysis of time resolved infrared transient absorption datasets indicates there to be no change during the lifetime of GFP_{I*} in frequency or amplitude of the 1711 cm^{-1} transient belonging to protonated glutamate 222.[33] The infrared anisotropy of the 1711 cm^{-1} transient does not change either during the lifetime of GFP_{I*} and GFP_{I2}, which was determined using photoselection measurements.[58] The constant anisotropy does not give an indication of a directional or specific change of the protonation state of carboxylate groups in GFP in the lifetime of the GFP_{I*} excited state, and transfer to glutamate 5, as proposed,[52,54] is not directly supported from this evidence which was obtained at room temperature with measurements out to 2 ns.[33] Fluorescence data that were analysed up to 15 ns may probe a subsequent phase in the photocycle. Such long delays are inaccessible for photoselection experiments under conditions where the delay approaches the rotational correlation time. However, with measurements in D_2O that allow transient accumulation of the GFP_{I2} ground state intermediate, changes of the COOD stretching mode are observed on longer time scales. With transient formation of the GFP_{I2} ground state intermediate which has a 5 ns lifetime,[51] a 7 cm^{-1} down-shift and reduced intensity is observed, indicating increased hydrogen bonding and a decreased protonation level, or transfer to another carboxylate group altogether.[33] This could be the proposed transfer to the glutamate 5 group[52,54] provided that its COOH vibrational transition dipole moment (TDM) aligns with that of Glu222 and thus does not lead to alteration of the infrared anisotropy.

An alternative possibility that could explain the changes in the COOH stretching region could be the rearrangement of the hydrogen bonding of the glutamate 222 carboxylate from the *anti*- to the *syn*-position. Brejc *et al.*[13] considered the possibility of *anti–syn* isomerisation of Glu222, but proposed that it occurs within the lifetime of the GFP_{I*} excited state, thereby breaking the hydrogen bonding between the COOH and the nearby Ser205.[13] In contrast, simulations did not lead to *anti–syn* isomerisation within the 100 ps time scale of the calculation.[42] Recent quantum dynamics calculations concluded that the proton wire between the chromophore and the Glu222 carboxylate must break up after the initial proton transfer event, and *anti–syn* isomerisation was suggested as a possibility.[45] The *anti*-to-*syn* rearrangement would however be expected to result in changes in the COOH/D stretching region within the lifetime of the excited state, which are not observed. The absorption changes are consistent with a single spectroscopic species during both the formation and the decay of the excited state GFP_{I*} from picoseconds to nanoseconds.[32,58] Changes in the COOD stretching frequency and intensity are observed only after its radiative decay or population dumping, with the formation of the GFP_{I2} ground state intermediate[32,58] (Fig. 6). A recent report proposed *anti–syn* isomerisation of Glu222 and disruption of the proton wire between the carboxylate and the chromophore to be part of the formation of the GFP_{I2} ground state intermediate.[67] In this work, the crystal structure of the Ser205Val mutant revealed a possible new hydrogen bonding network that could support ESPT, involving rearrangements of Glu222 and Thr203. The Thr203 side chain OH group was observed at a 3.3 Å distance from a crystallographic water that is H-bonded to the phenolic oxygen of the chromophore (PDB 2QLE), that contrasts with the 2.7 Å distance between the equivalent water–Ser205 distance in the H-bonding network observed in the wild type (PDB 1EMB;[13]). The increased distance is proposed to explain the $\sim$30 fold reduction in the rate of ESPT at room temperature in the Ser205Val mutant.[67] Consequently, the authors propose that a similar rearrangement of Thr203 and Glu222 may occur in the photocycle of the wild type, specifically upon formation of the relaxed GFP_{I2} ground state intermediate which forms with a 3 ps time constant from the GFP_{I1} precursor, and is associated with a moderate KIE of 2.[51]

The various proposals may be evaluated on the basis of the observed spectroscopic properties of the COOH stretching mode, in particular its frequency, intensity and anisotropy. An estimate can be made for the infrared anisotropy and resulting angle between optical and vibrational TDM for the proposed proton transfer to Glu5.[52,54] Assuming the site of protonation to be the OE2 oxygen of the Glu5 carboxylate (PDB 1W7S)[32] an angle of 69° would be predicted whereas the finite bleach corrected experimental measurement is 33° for both the GFP_{I*} excited state and GFP_I ground state intermediate.[58] DFT and TD-DFT calculations predict 27° for the COOH stretching mode of Glu222,[58] and thus the experimental data could be consistent with transfer to its

 This journal is © The Royal Society of Chemistry 2009

Published on 28 August 2009. Downloaded by Universitat Erlangen Nurnberg on 29/03/2016 08:56:33.

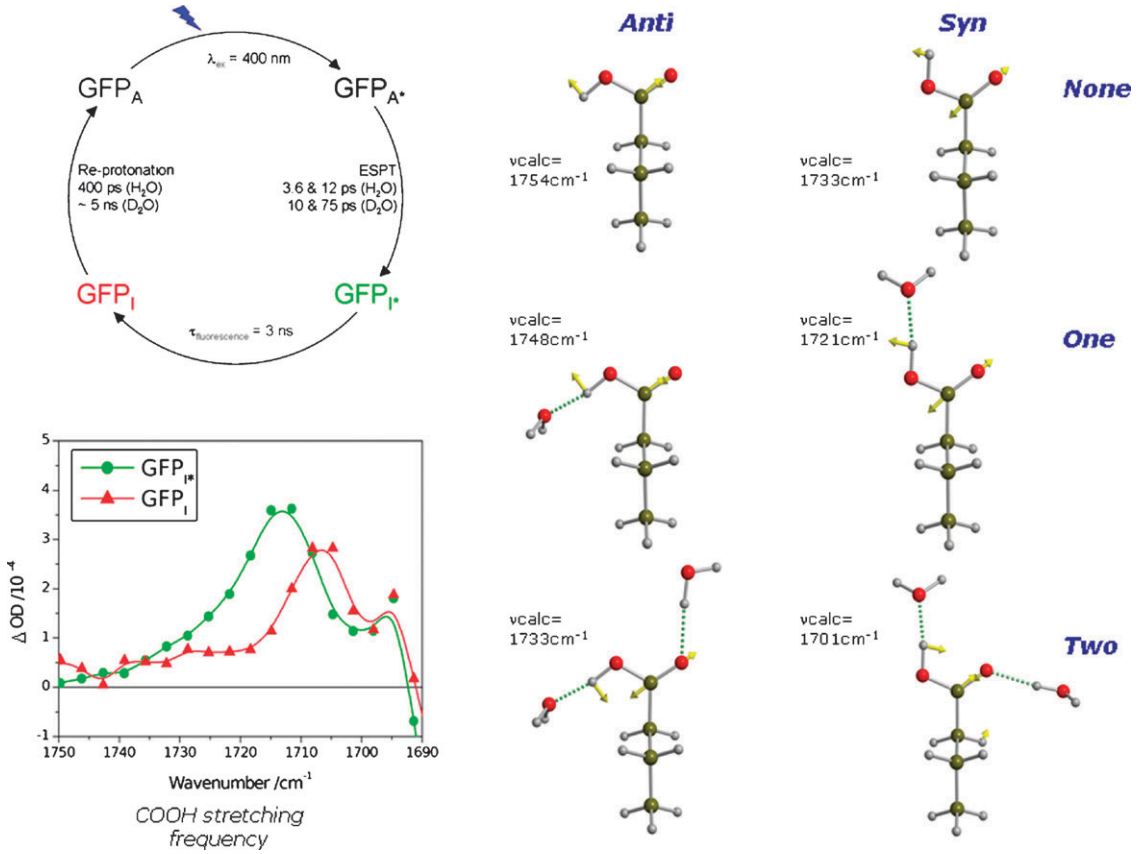

Fig. 6 Can the downshift of the COOD stretching mode in the $GFP_{I*} \rightarrow GFP_I$ transition be explained by *anti–syn* isomerisation of glutamate 222? Frequency calculations at the B3LYP/6-31G + (d,p) level are shown for minimised glutamate side chain structures with none, one and two hydrogen bonds with water in both *anti* and *syn* configurations. The calculations suggest that the downshifted frequency may be explained by *anti–syn* isomerisation, but likely with the number of hydrogen bonding interactions maintained, which are modelled here as interactions with waters. The inset shows the COOD stretching region of the species associated difference spectra belonging to GFP_{I*} and GFP_{I2}, relative to GFP_A; reproduced with permission.[32]

carboxylate only, up to 2 ns that sees the decay of GFP_{I*} and the rise of GFP_{I2} in D_2O but not its decay. IR measurements with longer delays would be required to determine whether an additional intermediate can be detected, that might involve proton transfer to Glu5, as proposed.[52,54]

The downshift of the COOD stretching frequency which occurs in the $GFP_{I*} \rightarrow GFP_I$ transition could alternatively signal changes in the configuration and interactions of the Glu222 side chain if no protonation change occur. It could either result from an increase of the hydrogen bonding strength or from a rearrangement such as the *anti–syn* isomerisation of the protonated carboxylic acid group. Frequency calculations at the B3LYP/6-31G + (d,p) level shown in Fig. 6 explore the effects of both. The associated vibrational TDM has very similar orientation in all configurations and could be consistent with the constant infrared anisotropy that was determined for both GFP_{I*} and GFP_I species.[58] The calculations indicate that isomerisation is expected to be associated with a measurable downshift of the stretching mode frequency (Fig. 6). However, if *anti–syn* isomerisation is accompanied by disruption of hydrogen bonding interactions to Glu222,[67] then there would be two opposing effects on the force constant of the stretching mode. The calculations shown in Fig. 6 nevertheless result in a 12 cm^{-1} overall downshift if one interaction is lost in the *anti–syn* transition, but the multiple approximations that are used should be taken into account.

Remarkably, formation of the GFP_I ground state intermediate by optical dumping of the GFP_{I*} state with a green pulse at 500 ps after GFP_A excitation forms the same species directly, also having a downshifted and reduced intensity COOD band.[33] This observation suggests that the excited state TDM has a direct and controlling influence on the protonation state of the proton acceptor. The downshifted COOD stretching frequency in the GFP_I state is evidence that is opposed to several proposals and theoretical results that include the disruption of the hydrogen bond between protonated Glu222 and Ser205 during the lifetime of the GFP_{I*} excited state or later in the photocycle.[13,45] In the absence of *anti–syn* isomerisation, the breakage of this hydrogen bond would be expected to upshift the COOH stretching frequency, whereas a downshift is observed.

Mutational analysis has provided insight into the molecular basis of the ESPT process (Fig. 7). The replacement of Glu222 with aspartate had a direct effect on the ESPT kinetics as well as on the level of ground state heterogeneity.[33,58] X-Ray crystallographic analysis of the Glu222 side chain has shown it to be disordered (Fig. 3),[33] and a correlation of weak and

Published on 28 August 2009. Downloaded by Universitat Erlangen Nurnberg on 29/03/2016 08:56:33.

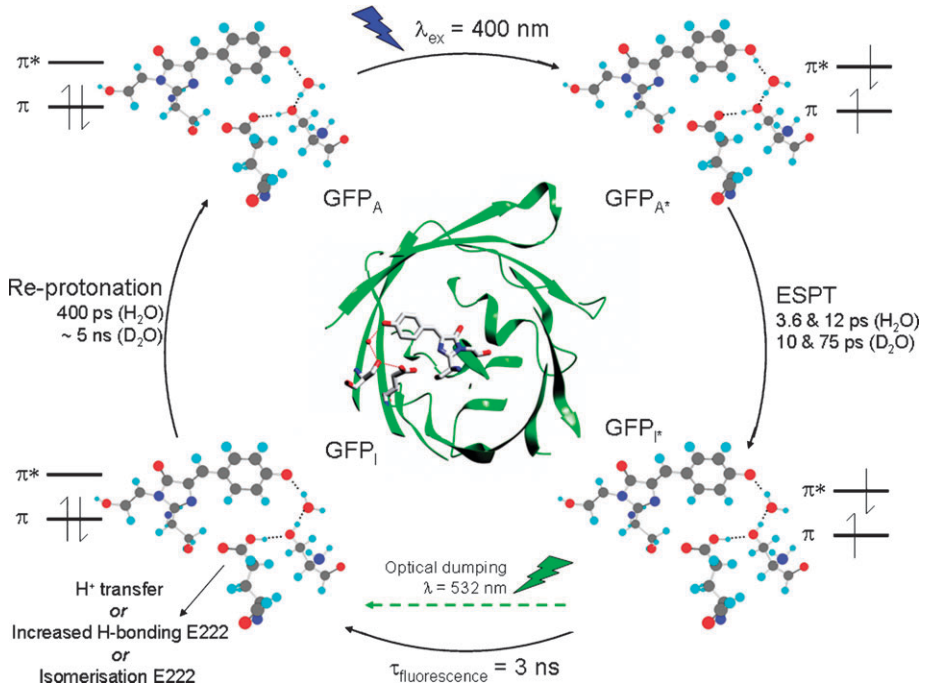

Fig. 7 Summary of the kinetics and proton transfer from the chromophore, to water, to serine 205 to glutamate 222 in the fluorescence photocycle of GFP with excitation of the dominant GFP_A neutral ground state species. The kinetic isotope effect (KIE) of the excited state proton transfer (ESPT) reaction is found to be ~5 from time resolved visible absorption, time resolved fluorescence and time resolved infrared measurements. The fluorescence lifetime of the anionic GFP_{I*} state is 3 ns in the wild type and optical dumping of the GFP_{I*} state efficiently populates the GFP_I electronic ground state. A large KIE of 12 is associated with the subsequent re-protonation of the chromophore to reform the GFP_A dark resting state, which could be consistent with multiple individual proton transfer steps through extended H-bonded chains as proposed,[52] or rearrangement of its hydrogen bonding and configuration. Figure adapted with permission from ref. 58.

strong hydrogen bonded populations with rapid and slow ESPT as argued above has been possible from the assignments for carboxylate stretching modes made on the basis of mutational analysis. More extensive re-wiring of the hydrogen bonding network resulted from a double mutation His148Asp/Ser65Thr.[23,67] The background mutation Ser65Thr is a commonly used modification that stabilises the anionic form of the chromophore, which has a higher cross-section but reduced fluorescence quantum yield relative to the neutral species.[68] Replacing His148 in this environment with an aspartic acid provides a nearby carboxylic acid that can hydrogen bond to the phenolic chromophore, and functional ESPT and red-shifted fluorescence emission was demonstrated at pH 6.9.[23] The rate of ESPT in this mutant was found to be much faster and occurs on the time scale of 170 fs.[69,70] X-Ray crystallographic analysis indicated a short hydrogen bond distance, less than 2.4 Å, and it was proposed to be low-barrier.[70] Another modification replaced Ser205 with a valine and thus removes the hydrogen bonding network between the chromophore phenolic oxygen and Glu222.[67] Nevertheless, ESPT was found to be operative in this mutant, although with an approximately 30 times slower rate constant than in the wild type. In the mutant Glu222 is reoriented and hydrogen bonded to Thr203, and ESPT is proposed to proceed *via* a water, Thr203 to Glu222.[67] In the double mutant Glu222Gln/His148Asp a situation occurs that is very similar to the His148Asp/Ser65Thr mutant, and green fluorescence is observed as the result of the second His148Asp mutation in the Ser65Thr background that stabilises the anionic chromophore.[63] Ultrafast infrared spectroscopy measurements of the His148Asp/Ser65Thr and the Glu222Gln/His148Asp mutants interestingly showed no absorption changes in the COOH region, ~1705 cm^{-1} for either sample,[63] in contrast to the wild type or the Glu222Asp mutant.[33] The existence of a barrierless hydrogen bond between the phenolic oxygen and Asp148 was proposed to account for this observation,[63] which is consistent with the conclusions based on X-ray crystallographic observation of a very short hydrogen bond and an ultrafast, 170 fs ESPT reaction.[69,70]

4 Vibrational mode analysis of GFP

Vibrational spectroscopy of GFP has greatly aided the assignment and characterisation of light induced transitions. Rigorous model compound and isotope substitution experiments in combination with normal mode analysis using density functional theory have provided some of the most solid assignments for chromophore modes that are available in biological Raman and IR spectroscopy.[17,31,71,72] As mentioned above, resonance Raman (RR) spectroscopy identified the neutral chromophore to be the dominant species which absorbs maximally at 400 nm in GFP.[17] Particularly powerful in this series of investigations was the systematic isotope substitutions in the HBDI model compound, including ^{13}C substitutions at positions α, 1, 3 and 5 and ^{15}N substitution of the imidazolinone nitrogen. For example,

 This journal is © The Royal Society of Chemistry 2009

Published on 28 August 2009. Downloaded by Universitat Erlangen Nurnberg on 29/03/2016 08:56:33.

these verified the assignment of the νCO stretching mode arising from the imidazolinone carbonyl group at 1744 (for the cation), 1697 cm^{-1} (for the neutral form), and 1665 cm^{-1} (for the anion).[72] Modes between $\sim$1150 and 1750 cm^{-1} could be assigned a major mode character for each ionised species, although with less success for the anionic species at the DFT/6-31G** level which did not include diffuse functions.[72] A reasonable correspondence was found between the mode character assigned on the basis of isotope substitutions and harmonic frequency calculations that used density functional theory[71,72] as opposed to calculations done at the Hartree Fock (HF) level.[73] Unfortunately the HF study did not report the mode character, only frequencies and intensities,[73] but it emerged that the mode character at the DFT level is substantially different for the free HBDI chromophore.[58,71,72] The DFT results are considered to be more accurate on the basis of the observed isotope shifts and Esposito *et al.*[71] additionally argued that the calculated intensities using DFT correspond more closely with experimental intensities. A separate computational approach used Car–Parrinello molecular dynamics simulations at the DFT level, where the Fourier transform of the auto-correlation function provides the mode density for the simulations, that were run up to 1.5 ps.[74] Surprisingly, no phenol ring contributions were reported from this procedure in the $\sim$1600–1500 cm^{-1} range, as expected and also concluded on the basis of harmonic frequency calculations by Esposito *et al.*[71]

Raman spectroscopy in the 1000–1660 cm^{-1} region has been reported for WT and Ser65Thr GFP mutants and for a model-chromophore molecule[31] The study correlates the frequencies of a particular mode in the 1610–1655 cm^{-1} range with the optical absorption energy in the cationic, neutral, and anionic forms of a model chromophore compound (ethyl 4-(4-hydroxyphenyl)methylidene-2-methyl-5-oxoimidazolacetate), the anionic (but not the cationic) form of the chromophore in various solvents, wild-type GFP, and the Ser65Thr mutant. The authors propose that a shift in the Raman bands may reflect a change in the stabilisation of the ground state, which may in turn dominate the optical absorption shifts.[31]

FTIR difference spectroscopy observed the difference spectrum of wild type GFP of the anionic species minus the neutral ground state species in the 1000–1800 cm^{-1} region in H_2O and D_2O.[22] Prominent marker modes identified deprotonation of the phenolic ring in the phototransformation process. Respective up- and down-shifts upon phenol ring deprotonation of specific vibrational modes are well documented,[75,76] and observed in GFP at 1518 and 1244 cm^{-1} for the protonated phenol ring and are shifted to 1498 and 1270 cm^{-1} upon deprotonation.[22]

The vibrational response of the chromophore in the fluorescence photocycle has been addressed by a number of time-resolved infrared measurements.[32,33,58,59,62] Assignments of the GFP_A ground state modes have been proposed on the basis of the aforementioned isotope substitution and DFT calculation approach.[17,71,72] Additionally, transient accumulation of the GFP_I electronic ground state in D_2O allowed identification of anionic markers in the late photocycle intermediate. With regard to the GFP_{A*} and GFP_{I*} excited state modes, proposed assignments were initially based on expected downshifts from reduced bond orders,[33] and subsequently on the basis of configuration interaction singles (CIS) excited state frequency calculations.[58] With regard to chromophore modes additional experimental evidence was found from photoselection experiments, reported for some ground state modes[62] and for all photocycle intermediates, including electronically excited states.[58] Without discussing specific modes, the general conclusion is that a selected set of vibrational modes exhibited good correspondence between experimental and theoretical dichroism, whereas there were discrepancies for others.[58] The theoretical calculations were done at the B3LYP level for the isolated chromophore and assessed the vibrational transition dipole moments from both numerical and analytical procedures in the harmonic approximation.[58] This raises questions with respect to the accuracy of the mode character that is obtained from such calculations, and prompts the use of approaches that include the specific protein environment. For example, geometry optimisation of rhodopsin was performed using a three layer ONIOM hybrid scheme with a ONIOM(QM-high:QM-low:MM) approach.[77] Extending such calculations to excited states however would require development of the necessary theory extensions and code that currently do not exist. Deviations from calculated vibrational transition dipole moment vectors and experimental dichroism may result from not yet having included the direct environment. However, displacements of modes that are discussed in the mid-infrared region are likely to be in the plane of the chromophore and the sensitivity to the chromophore environment with respect to mode character and the dipole response is difficult to predict.

One chromophore mode in particular has been subject of discussion because it may be used to probe torsional motion of the free HBDI chromophore in solution. Theoretical calculations indicated the presence of an intersection between excited and ground state potentials for twisted geometries of the chromophore leading to the proposal that such excited state twisting is the dominant deactivation channel that is inhibited in the intact protein.[26] Experimental evidence for such twisting was sought by probing the time-resolved anisotropy changes of a localised reporter mode by preparing the sample using linearly polarised pulses.[78] The stretching mode of the imidazolinone C=O, for the neutral state absorbing near 1680 cm^{-1} is relatively localised but has contributions from C=C stretching (Fig. 8). Usman *et al.* probed the transient anisotropy of this mode with photoselection using linearly polarised femtosecond visible excitation.[78] An unexpected observation for the excited state was the upshifted and broad induced absorption that was assigned to the C=O mode for the free chromophore[78] that is not observed for the GFP_{A*} excited state in the intact protein. In GFP, the excited state C=O mode is proposed to be downshifted on the basis of expected bond order reduction, CIS frequency calculation and photoselection measurements.[58] In contrast, in free HBDI a broad and kinetically uncoupled upshifted feature at $\sim$1750 cm^{-1} is assigned to the excited state frequency of the mode, which would indicate a substantially different excited state behaviour that was interpreted to arise from formation of a charge transfer state.[78] For both neutral and cationic HBDI

Published on 28 August 2009. Downloaded by Universitat Erlangen Nurnberg on 29/03/2016 08:56:33.

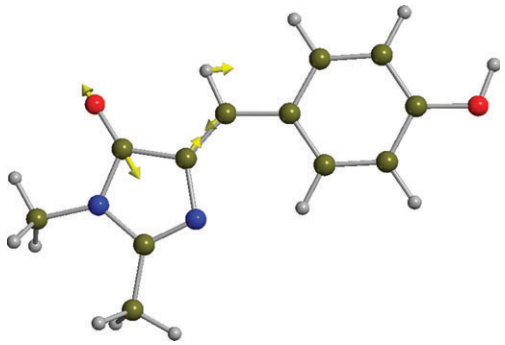

Fig. 8 An important spectator mode for vibrational spectroscopy of GFP and HBDI. The normal mode displacements of the 'C=O' stretching mode of HBDI are shown as arrows. Harmonic frequency calculations indicate a mixed C=O and C=C stretching character, that is sensitive to electronic excitation. In the GFP_A ground state its frequency is 1685 cm^{-1}.[22]

the measurements provided angles of 70° and 52° between the optical and C=O vibrational transition dipole moment in S0 and S1, respectively. Assuming that the vibrational TDM lies along the CO bond vector, the results could reflect either single bond rotation by 120° or a hula twist of 150°.[78] In contrast, in the intact protein no equivalent upshifted signal is observed in S1, and the assignment was proposed for a downshifted absorption.[58] Specifically, a variation of the anisotropy was observed across the bleach present in the $GFP_{A*} - GFP_A$ difference spectrum, that was interpreted to result from a downshift and reduced cross-section of the mode. According to this interpretation, the experimental data may also suggest a reduced angle between the optical and the C=O vibrational TDM in the intact protein,[58] as has been argued for HBDI.[78] Calculation of TDM vectors provides an alternative explanation that does not require excited state twisting. Fixing the geometry of the HBDI chromophore to a planar configuration in both the S0 and S1 states, calculations at the HF and CIS level indicate a decrease of the angle between the vibrational and optical TDM. The primary difference between the S0 and S1 harmonic frequency calculations is a change of the C=O and C=C stretch (Fig. 8) mode mixing due to bond softening in S1, which results in a changed dipole response that may explain the experimental observations for both the isolated HBDI chromophore[78] and the intact protein,[58] without the need to invoke excited state twisting.

The low frequency torsional modes of the chromophore are of special interest, particularly because these are proposed to be linked to deactivation mechanisms. An important spectroscopic observation compares the line shape and width of the fluorescence spectra of the intact protein and the anionic HBDI model compound in solution.[79] At reduced temperatures, the emission from the intact protein is characterised by vibronic features and a narrow line shape whereas HBDI in solution shows a broad featureless line shape. Stavrov *et al.* have put forward that torsional deformation contributes to the temperature dependence of the fluorescence.[79] Furthermore, it was shown that the line shape of HBDI may be fitted by convolution of the structured intact protein spectrum with a function that describes the normal distribution of the transition energy of HBDI. Consequently it was argued that the line broadening and deactivation in HBDI are through torsional deformation of the phenyl bond.[79]

A strong focus of many structural, spectroscopic and theoretical studies has been the explicit role of the protein environment in the photoreactions of GFP. Vibrational spectroscopy has probed the vibrational response of protein groups in the fluorescence and phototransformation pathways. Besides the assignment of the transient at ~1711/1725 cm^{-1} to COOD/COOH of Glu222, additional infrared absorption changes have been attributed to individual amino acids. Particularly, a transient at 1697 cm^{-1} could be assigned to Gln69 C=O stretching, from the FTIR analysis of a Thr203His/Gln69Leu mutant and X-ray crystallography of intermediates in the phototransformation pathway.[32] Time-resolved measurements showed the perturbation of the Gln69 side chain to occur on the picosecond time scale in the fluorescence photocycle from the transient absorption at 1697 cm^{-1}.[32,33] To the best of our knowledge the observation of a sub-picosecond response of the Gln69 side chain represents the fastest that is documented of individual amino acids in an intact protein. The ultrafast protein response is not necessarily a unique feature of GFP, but in this instance detailed assignments of individual protein groups are available on the ultrafast time scale. For example, in proteorhodopsin sub-picosecond protein dynamics have been detected from the vibrational response of the Amide II mode, reporting on ultrafast protein backbone conformational dynamics.[80] Additional signals attributed to amino acids include a Cys70 S–H stretching vibration observed at 2552 cm^{-1} by cryo-trapping after phototransformation, but which has not yet been detected on the picosecond or nanosecond time scales possibly because its amplitude is below the available S/N for pump–probe experiments. The role of the rapid amino acid response in the fluorescence photocycle has been discussed.[32] It was proposed, additionally on the basis of the low fluorescence quantum yield of the Thr203His/Gln69Leu mutant, that the rapid amino acid motions may inhibit internal recombination by stabilisation of the GFP_{I*} excited state.[32] Specifically, the structural rearrangements of the protein environment that were observed by infrared spectroscopy and X-ray crystallography of cryo-trapped photointermediates could accommodate the rapid electrostatic changes that are induced by chromophore photoionisation, and are proposed to stabilise the radiative state.[32] This conclusion is also supported by theoretical[81–83] and Stark spectroscopy[11,84] studies and suggests that charge transfer is linked to the large frequency separation between excitation and emission and the bright fluorescence of GFP.

5 Phototransformation

Other remarkable features of GFP include the autocatalytic formation of its chromophore, that is not discussed here, and its photochromic properties, that were later also discovered in other fluorescent proteins. It was observed that during prolonged optical excitation of the GFP_A state at 400 nm using pulsed lasers, the bulk absorption progressively changes to reflect the accumulation of a photoproduct that has an

 This journal is © The Royal Society of Chemistry 2009

Published on 28 August 2009. Downloaded by Universitat Erlangen Nurnberg on 29/03/2016 08:56:33.

anionic chromophore and has an absorption redshifted by ~80 nm.[11,85] This photochromic process occurs with low quantum yield and was initially reported to be thermally reversible.[11] In contrast, measurements done after photoconversions indicated only very small, less than 1%, absorption changes of the anionic photoproduct occurring on the time scale of days and conversion was found to be essentially irreversible.[22] Such very small absorption changes are reminiscent of conversion between neutral GFP_A and anionic GFP_B such as those caused by dilution or ionic strength[1,34] and probably reflect slow protein relaxation such as dimerisation that is linked to pK_a changes of the chromophore. In support of this possibility, the X-ray structure of the photoproduct revealed dimer contacts that are different from those in the unconverted dark form.[86]

The thermal reversibility reported by Chattoraj *et al.*[11] led to proposals for possible molecular explanations for the reversible mechanism. One particular and commonly referenced proposal involves a mechanism whereby rearrangement of the hydrogen bonding network between the chromophore and glutamate 222 was expected to form a metastable phototransformed species.[13] Specifically, an *anti* to *syn* rearrangement of protonated glutamate 222 in the excited GFP_{I*} state was proposed to explain the slow thermal return to GFP_A that was reported by Chattoraj *et al.*[11,13] Explicit electrostatic calculations that explored this model in molecular detail supported this proposal and provided an estimation of the stabilisation energy of the presumed stabilised anionic species that appeared to fit the reported kinetics.[14] However, it emerged that the photochromic reaction was fully irreversible and involves covalent modification triggered by electron transfer.[12]

An X-ray crystallographic investigation of the purified stable photoproduct of GFP revealed a change in the active site relative to the ground state. No electron density was observed for the carboxylate side chain of glutamate 222 and mass spectrometry indicated that illumination reduces the mass of the polypeptide by 44 Da, providing evidence for the light induced decarboxylation of the side chain[12] (Fig. 9). GFP is the only known example where glutamate acts as an electron donor during functional turnover in a protein, albeit as a side reaction with relatively low quantum yield—up to 3%. Mass spectrometry proved that both blue excitation at 390 nm and UV excitation at 254 nm triggers electron transfer, but with increased quantum yield for short wavelength excitation (Fig. 2). Low temperature ESR experiments indicated that no radical species accumulates during photoconversion of the bulk, prompting the possibility of recombination by electron and proton transfer from the chromophore (Fig. 9).

The singlet excited state is the one photon generated oxidant for the decarboxylation reaction and the absence of additional intermediates is based on the experimental observation that the photoconversion rate constant in bulk depends linearly on the power density used. This relationship was established with ~7 ns pulses at 390 nm,[12] but has not yet been investigated in detail outside this regime, although it is clear that phototransformation also occurs with femtosecond optical excitation as well as with cw illumination. Assuming a parallel model, the electron transfer rate is taken from the quantum yield of photoconversion to be $2.4 \times 10^8\ s^{-1}$, which is argued[64] to be low in view of the near van der Waals distance between the carboxylate electron donor and the excited chromophore electron acceptor. The wavelength dependence of the transformation, which shows an increased quantum yield for short wavelength excitation (Fig. 2), is understood from the increased free energy and assumes a one photon transition. A different proposal put that the wavelength dependence results from two-photon excitation of the chromophore at visible wavelengths,[87] which is inconsistent with established behaviour, notably the linear variation of the phototransformation rate with intensity using pulsed excitation at 390 nm[87] and with phototransformation occurring with continuous illumination at 413 nm.[32]

The charge migration in the excited state thus has multiple consequences, including the photoacid nature of the chromophore. There can additionally be a contribution to electron transfer in addition to the electron spin pairing of the unpaired electron left in the valence shell. Stark spectroscopy has probed the neutral GFP_A and anionic GFP_B states and has provided insight into the change in transition moment associated with the ultrafast deprotonation.[11,84] The studies indicated that the Stark effect is dominated by the change in dipole moment and it was concluded that a charge transfer between the phenolic and imidazolinone oxygens explains the data well.[11,84] Interestingly, it was shown that excitation of GFP_A leads to a relatively small charge displacement whereas excitation of GFP_B results in a much larger change. The

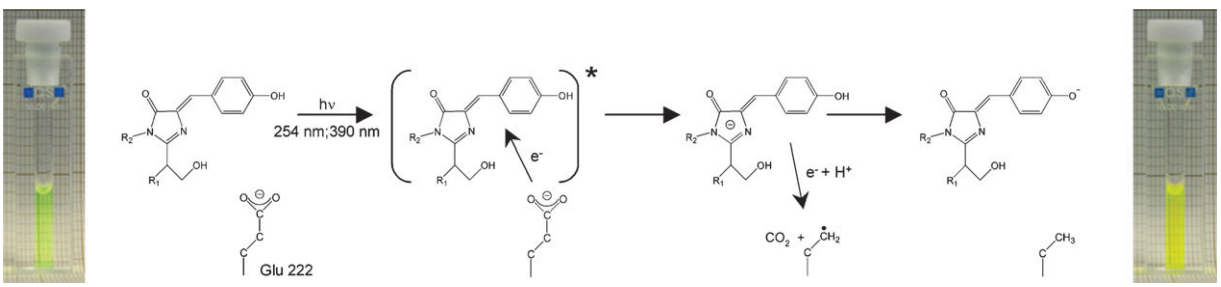

Fig. 9 Light induced electron transfer to the electron deficient chromophore in the GFP_{A*} state results in oxidation of the COO^- carboxylate side chain of glutamate 222, which forms an unstable radical from which a CO_2 molecule is cleaved off irreversibly according to the 'Kolbe' mechanism. By disrupting the hydrogen bonding network shown in Fig. 3 for the ground state, the neutral species becomes destabilised, causing a pronounced colour change. Reproduced with permission.[12]

Published on 28 August 2009. Downloaded by Universitat Erlangen Nurnberg on 29/03/2016 08:56:33.

directions of the excited state dipoles for GFP_{A*} and GFP_{B*} were found to be close in spite of the difference in ionisation state, on the basis of which was argued that protein relaxation akin to solvation processes occur during the picosecond time scale associated with ESPT at room temperature.[84] Protein relaxation processes triggered by ESPT and by photoconversion, both involving ionisation of the chromophore phenolic oxygen, were experimentally found to resemble each other, particularly from the observation of structural perturbation of the Gln69 side chain.[32] A cryo-trapping approach probed the structural and spectroscopic relaxation processes that occur thermally after the initial photoionisation event. The X-ray structures and cryo-FTIR difference spectra of intermediates determined at 100, 170 and 293 K showed discrete stages of short range and long range structural relaxation processes, and these identified those occurring in the chromophore binding site including Gln69 perturbation to have very a low barrier, consistent with the observation of a picosecond time constant at ambient temperature.[32]

Photoinduced electron transfer and isomerisation reactions have been identified in a number of fluorescent proteins. For instance, a decarboxylation event responsible for a colour change in the red-emitting variant DsRed has been documented[88] and photoinduced breaks in the peptide chains adjacent to the chromophore associated with the green-to-red spectral shift in Kaede and EosFP.[89–91] Additionally, a *cis–trans* photoisomerisation of the chromophore activates the fluorescence of an initially non-fluorescent mutant of the kindling fluorescent protein (KFP)[92] and is at the basis of photoconversion of variants of a red fluorescent protein eqFP611.[93,94] A discussion of the details and all examples of photoactivation reactions in other fluorescent proteins is outside the scope of this review.

The phototransformation mechanism has been exploited for fluorescence microscopy approaches that used localised laser irradiation to label, or 'highlight' specific regions with the anionic photoproduct, allowing spatial and temporal monitoring of particular populations in cells. Increased spectroscopic contrast has been achieved and used by using a Thr203His mutant that in the ground state at neutral pH is exclusively present in the neutral GFP_A state, so that photoconversion results in a more pronounced increase in the fluorescence signal with excitation near 480 nm that is resonant with the anionic ground state species.[95] The Thr203His mutant is also known as the 'photoactivatable GFP' or 'PA-GFP', and it was recently confirmed from X-ray crystallographic analysis that the photoconversion mechanism is the same as in the wild type and involves light induced decarboxylation of Glu222.[96] The light activation of specific populations of 'PA-GFP' allowed as first examples the measurement of protein diffusion across the nuclear envelope and inter-lysosomal membrane exchange in COS cells.[95] Photoactivation of sub-populations of 'PA-GFP' is also used in developments that allow 'super-resolution' microscopy that breaks the diffraction limit.[97–99] The technique of 'photoactivated localisation microscopy (PALM)' is capable of providing spatial resolution of a few nanometres, and relies on localisation of individual molecules by determining the center of fluorescence by a statistical fit of the point spread function that defines the diffraction limited resolution limit of the optical system.[97,98] PA-GFP is well suited for this approach. A quantum yield of a few percent allows controlled formation, and in multiple cycles, of appropriate populations of photoconverted GFP. The spectroscopic contrast with green excitation of the anionic photoproduct is very high and both subsequent imaging and bleaching that is required to be able to initiate another cycle is therefore highly specific for the photoactivated species. Undoubtedly, biological research will benefit tremendously from the newly developed high resolution microscopy imaging and photoactivation methodologies.[95,97,98,100–106]

6 Conclusion

This review highlights some of the most exciting discoveries and research on the wild type GFP that seek to understand and probe its numerous remarkable features. GFP has electrified scientific communities ranging from biology, chemistry, medicine and physics and is continuing to do so. The now extended family of fluorescent proteins is providing a palette of spectroscopic and physical properties for many different applications, and the wild type *A. victoria* GFP serves as a blueprint for understanding their functions. In this present contribution a particular interest is evident in the specificity of the protein environment and protein dynamics and the dramatic nature of the ultrafast charge rearrangements that are triggered. GFP also provides a laboratory for entangling principles of protein function, particularly with a view to structural dynamics, that has broad impact and relevance.

References

1 R. Y. Tsien, *Annu. Rev. Biochem.*, 1998, **67**, 509–544.
2 R. Heim, D. C. Prasher and R. Y. Tsien, *Proc. Natl. Acad. Sci. U. S. A.*, 1994, **91**, 12501–12504.
3 C. W. Cody, D. C. Prasher, W. M. Westler, F. G. Prendergast and W. W. Ward, *Biochemistry*, 1993, **32**, 1212–1218.
4 F. Yang, L. G. Moss and G. N. Phillips, Jr, *Nat. Biotechnol.*, 1996, **14**, 1246–1251.
5 M. Ormo, A. B. Cubitt, K. Kallio, L. A. Gross, R. Y. Tsien and S. J. Remington, *Science*, 1996, **273**, 1392–1395.
6 N. C. Shaner, G. H. Patterson and M. W. Davidson, *J. Cell Sci.*, 2007, **120**, 4247–4260.
7 S. J. Remington, *Curr. Opin. Struct. Biol.*, 2006, **16**, 714–721.
8 A. A. Pakhomov and V. I. Martynov, *Chem. Biol.*, 2008, **15**, 755–764.
9 H. Niwa, S. Inouye, T. Hirano, T. Matsuno, S. Kojima, M. Kubota, M. Ohashi and F. I. Tsuji, *Proc. Natl. Acad. Sci. U. S. A.*, 1996, **93**, 13617–13622.
10 N. M. Webber, K. L. Litvinenko and S. R. Meech, *J. Phys. Chem. B*, 2001, **105**, 8036–8039.
11 M. Chattoraj, B. A. King, G. U. Bublitz and S. G. Boxer, *Proc. Natl. Acad. Sci. U. S. A.*, 1996, **93**, 8362–8367.
12 J. J. van Thor, T. Gensch, K. J. Hellingwerf and L. N. Johnson, *Nat. Struct. Biol.*, 2002, **9**, 37–41.
13 K. Brejc, T. K. Sixma, P. A. Kitts, S. R. Kain, R. Y. Tsien, M. Ormo and S. J. Remington, *Proc. Natl. Acad. Sci. U. S. A.*, 1997, **94**, 2306–2311.
14 C. Scharnagl, R. Raupp-Kossmann and S. F. Fischer, *Biophys. J.*, 1999, **77**, 1839–1857.
15 T. M. Creemers, A. J. Lock, V. Subramaniam, T. M. Jovin and S. Volker, *Nat. Struct. Biol.*, 1999, **6**, 557–560.
16 G. J. Palm, A. Zdanov, G. A. Gaitanaris, R. Stauber, G. N. Pavlakis and A. Wlodawer, *Nat. Struct. Biol.*, 1997, **4**, 361–365.

 This journal is © The Royal Society of Chemistry 2009

Published on 28 August 2009. Downloaded by Universitat Erlangen Nurnberg on 29/03/2016 08:56:33.

17 P. Schellenberg, E. Johnson, A. P. Esposito, P. J. Reid and W. W. Parson, *J. Phys. Chem. B*, 2001, **105**, 5316–5322.
18 S. H. Bokman and W. W. Ward, *Biochem. Biophys. Res. Commun.*, 1981, **101**, 1372–1380.
19 M. Kneen, J. Farinas, Y. Li and A. S. Verkman, *Biophys. J.*, 1998, **74**, 1591–1599.
20 W. W. Ward, C. W. Cody, R. C. Hart and M. J. Cormier, *Photochem. Photobiol.*, 1980, **31**, 611–615.
21 H. Morise, O. Shimomura, F. H. Johnson and J. Winant, *Biochemistry*, 1974, **13**, 2656–2662.
22 J. J. van Thor, A. J. Pierik, I. Nugteren-Roodzant, A. Xie and K. J. Hellingwerf, *Biochemistry*, 1998, **37**, 16915–16921.
23 M. A. Elsliger, R. M. Wachter, G. T. Hanson, K. Kallio and S. J. Remington, *Biochemistry*, 1999, **38**, 5296–5301.
24 A. A. Voityuk, M. E. Michel-Beyerle and N. Rosch, *Chem. Phys. Lett.*, 1997, **272**, 162–167.
25 A. A. Voityuk, M. E. Michel-Beyerle and N. Rosch, *Chem. Phys. Lett.*, 1998, **296**, 269–276.
26 W. Weber, V. Helms, J. A. McCammon and P. W. Langhoff, *Proc. Natl. Acad. Sci. U. S. A.*, 1999, **96**, 6177–6182.
27 V. Helms, C. Winstead and P. W. Langhoff, *J. Mol. Struct.*, 2000, **306**, 179–189.
28 R. M. Dickson, A. B. Cubitt, R. Y. Tsien and W. E. Moerner, *Nature*, 1997, **388**, 355–358.
29 C. Blum and V. Subramaniam, *Anal. Bioanal. Chem.*, 2009, **393**, 527–541.
30 J. El Yazal, F. G. Prendergast, D. E. Shaw and Y. P. Pang, *J. Am. Chem. Soc.*, 2000, **122**, 11411–11415.
31 A. F. Bell, X. He, R. M. Wachter and P. J. Tonge, *Biochemistry*, 2000, **39**, 4423–4431.
32 J. J. van Thor, G. Y. Georgiev, M. Towrie and J. T. Sage, *J. Biol. Chem.*, 2005, **280**, 33652–33659.
33 J. J. van Thor, G. Zanetti, K. L. Ronayne and M. Towrie, *J. Phys. Chem. B*, 2005, **109**, 16099–16108.
34 W. W. Ward, H. J. Prentice, A. F. Roth, C. W. Cody and S. C. Reeves, *Photochem. Photobiol.*, 1982, **35**, 803–808.
35 A. Kohen and J. P. Klinman, *Chem. Biol.*, 1999, **6**, R191–198.
36 P. Leiderman, R. Gepstein, I. Tsimberov and D. Huppert, *J. Phys. Chem. B*, 2008, **112**, 1232–1239.
37 L. I. Trakhtenberg and V. L. Klochikhin, *Chem. Phys.*, 1998, **232**, 175–182.
38 P. Hanggi, P. Talkner and M. Borkovec, *Rev. Mod. Phys.*, 1990, **62**, 251–341.
39 R. C. Tolman, *J. Am. Chem. Soc.*, 1920, **42**, 2506–2528.
40 D. G. Truhlar and A. Kohen, *Proc. Natl. Acad. Sci. U. S. A.*, 2001, **98**, 848–851.
41 T. Ebata, A. Iwasaki and N. Mikami, *J. Phys. Chem. A*, 2000, **104**, 7974–7979.
42 M. A. Lill and V. Helms, *Proc. Natl. Acad. Sci. U. S. A.*, 2002, **99**, 2778–2781.
43 O. Vendrell, R. Gelabert, M. Moreno and J. M. Lluch, *Chem. Phys. Lett.*, 2004, **396**, 202–207.
44 O. Vendrell, R. Gelabert, M. Moreno and J. M. Lluch, *J. Am. Chem. Soc.*, 2006, **128**, 3564–3574.
45 O. Vendrell, R. Gelabert, M. Moreno and J. M. Lluch, *J. Phys. Chem. B*, 2008, **112**, 5500–5511.
46 T. Förster, *Naturwissenschaften*, 1949, **36**, 186.
47 T. Förster, *Z. Electrochem.*, 1950, **54**, 531.
48 L. M. Tolbert and K. M. Solntsev, *Acc. Chem. Res.*, 2002, **35**, 19–27.
49 Z. Smedarchina, W. Siebrand, A. Fernandez-Ramos and Q. Cui, *J. Am. Chem. Soc.*, 2003, **125**, 243–251.
50 E. Pollak and P. Talkner, *Chaos*, 2005, **15**, 26116.
51 J. T. Kennis, D. S. Larsen, I. H. van Stokkum, M. Vengris, J. J. van Thor and R. van Grondelle, *Proc. Natl. Acad. Sci. U. S. A.*, 2004, **101**, 17988–17993.
52 N. Agmon, *Biophys. J.*, 2005, **88**, 2452–2461.
53 P. Leiderman, M. Ben-Ziv, L. Genosar, D. Huppert, K. M. Solntsev and L. M. Tolbert, *J. Phys. Chem. B*, 2004, **108**, 8043–8053.
54 P. Leiderman, D. Huppert and N. Agmon, *Biophys. J.*, 2006, **90**, 1009–1018.
55 D. Huppert, P. Leiderman, M. Ben-Ziv, L. Genosar and L. Cohen, *J. Phys. Chem. B*, 2005, **109**, 4241–4251.
56 N. Agmon, *J. Phys. Chem. B*, 2007, **111**, 7870–7878.
57 R. Gepshtein, P. Leiderman and D. Huppert, *J. Phys. Chem. B*, 2008, **112**, 7203–7210.
58 J. J. van Thor, K. L. Ronayne, M. Towrie and J. T. Sage, *Biophys. J.*, 2008, **95**, 1902–1912.
59 D. Stoner-Ma, A. A. Jaye, P. Matousek, M. Towrie, S. R. Meech and P. J. Tonge, *J. Am. Chem. Soc.*, 2005, **127**, 2864–2865.
60 H. Lossau, A. Kummer, R. Heinecke, F. Pollinger-Dammer, C. Kompa, G. Bieser, T. Jonsson, C. M. Silva, M. M. Yang, D. C. Youvan and M. E. Michel-Beyerle, *Chem. Phys.*, 1996, **213**, 1–16.
61 K. Winkler, J. Lindner, V. Subramanian, T. M. Jovin and P. Vohringer, *Phys. Chem. Chem. Phys.*, 2002, **4**, 1072–1081.
62 D. Stoner-Ma, E. H. Melief, J. Nappa, K. L. Ronayne, P. J. Tonge and S. R. Meech, *J. Phys. Chem. B*, 2006, **110**, 22009–22018.
63 D. Stoner-Ma, A. A. Jaye, K. L. Ronayne, J. Nappa, S. R. Meech and P. J. Tonge, *J. Am. Chem. Soc.*, 2008, **130**, 1227–1235.
64 J. J. van Thor and J. T. Sage, *Photochem. Photobiol. Sci.*, 2006, **5**, 597–602.
65 R. Zhang, M. T. Nguyn and A. Ceuleman, *Chem. Phys. Lett.*, 2005, **404**, 250–256.
66 S. Wang and S. C. Smith, *J. Phys. Chem. B*, 2004, **110**, 19812–19817.
67 X. Shu, P. Leiderman, R. Gepshtein, N. R. Smith, K. Kallio, D. Huppert and S. J. Remington, *Protein Sci.*, 2007, **16**, 2703–2710.
68 R. Heim, A. B. Cubitt and R. Y. Tsien, *Nature*, 1995, **373**, 663–664.
69 X. Shi, P. Abbyad, X. Shu, K. Kallio, P. Kanchanawong, W. Childs, S. J. Remington and S. G. Boxer, *Biochemistry*, 2007, **46**, 12014–12025.
70 X. Shu, K. Kallio, X. Shi, P. Abbyad, P. Kanchanawong, W. Childs, S. G. Boxer and S. J. Remington, *Biochemistry*, 2007, **46**, 12005–12013.
71 A. P. Esposito, P. Schellenberg, W. W. Parson and P. J. Reid, *J. Mol. Struct.*, 2001, **569**, 25–41.
72 X. He, A. F. Bell and P. Tonge, *J. Phys. Chem. B*, 2002, **106**, 6056–6066.
73 H. Y. Yoo, J. A. Boatz, V. Helms, J. A. McCammon and P. W. Langhoff, *J. Phys. Chem. B*, 2001, **105**, 2850–2857.
74 V. Tozzini and R. Nifosi, *J. Phys. Chem. B*, 2001, **105**, 5797–5803.
75 Y. Imamoto, K. Mihara, O. Hisatomi, M. Kataoka, F. Tokunaga, N. Bojkova and K. Yoshihara, *J. Biol. Chem.*, 1997, **272**, 12905–12908.
76 K. J. Rothschild, P. Roepe, P. L. Ahl, T. N. Earnest, R. A. Bogomolni, S. K. Das Gupta, C. M. Mulliken and J. Herzfeld, *Proc. Natl. Acad. Sci. U. S. A.*, 1986, **83**, 347–351.
77 K. F. Hall, T. Vreven, M. J. Frisch and M. J. Bearpark, *J. Mol. Biol.*, 2008, **383**, 106–121.
78 A. Usman, O. F. Mohammed, E. T. Nibbering, J. Dong, K. M. Solntsev and L. M. Tolbert, *J. Am. Chem. Soc.*, 2005, **127**, 11214–11215.
79 S. S. Stavrov, K. M. Solntsev, L. M. Tolbert and D. Huppert, *J. Am. Chem. Soc.*, 2006, **128**, 1540–1546.
80 J. J. Amsden, J. M. Kralj, L. R. Chieffo, X. Wang, S. Erramilli, E. N. Spudich, J. L. Spudich, L. D. Ziegler and K. J. Rothschild, *J. Phys. Chem. B*, 2007, **111**, 11824–11831.
81 A. Sinicropi, T. Andruniow, N. Ferre, R. Basosi and M. Olivucci, *J. Am. Chem. Soc.*, 2005, **127**, 11534–11535.
82 M. E. Martin, F. Negri and M. Olivucci, *J. Am. Chem. Soc.*, 2004, **126**, 5452–5464.
83 P. Altoe, F. Bernardi, M. Garavelli, G. Orlandi and F. Negri, *J. Am. Chem. Soc.*, 2005, **127**, 3952–3963.
84 G. U. Bublitz and S. G. Boxer, *Annu. Rev. Phys. Chem.*, 1997, **48**, 213–242.
85 G. Striker, V. Subramaniam, C. A. M. Seidel and A. Volkmer, *J. Phys. Chem. B*, 1999, **103**, 8612–8617.
86 J. J. van Thor, T. Gensch, K. J. Hellingwerf and L. N. Johnson, in *The Proceedings of the 12th International Symposium on Bioluminescence (BL) and Chemiluminescence*, ed. Philip E. Stanley and Larry J. Kricka, 2002, pp. 119–122.
87 A. F. Bell, D. Stoner-Ma, R. M. Wachter and P. J. Tonge, *J. Am. Chem. Soc.*, 2003, **125**, 6919–6926.
88 S. Habuchi, M. Cotlet, T. Gensch, T. Bednarz, S. Haber-Pohlmeier, J. Rozenski, G. Dirix, J. Michiels, J. Vanderleyden,

Published on 28 August 2009. Downloaded by Universitat Erlangen Nurnberg on 29/03/2016 08:56:33.

J. Heberle, F. C. De Schryver and J. Hofkens, *J. Am. Chem. Soc.*, 2005, **127**, 8977–8984.
89 I. Hayashi, H. Mizuno, K. I. Tong, T. Furuta, F. Tanaka, M. Yoshimura, A. Miyawaki and M. Ikura, *J. Mol. Biol.*, 2007, **372**, 918–926.
90 H. Mizuno, T. K. Mal, K. I. Tong, R. Ando, T. Furuta, M. Ikura and A. Miyawaki, *Mol. Cell*, 2003, **12**, 1051–1058.
91 K. Nienhaus, G. U. Nienhaus, J. Wiedenmann and H. Nar, *Proc. Natl. Acad. Sci. U. S. A.*, 2005, **102**, 9156–9159.
92 M. Andresen, M. C. Wahl, A. C. Stiel, F. Grater, L. V. Schafer, S. Trowitzsch, G. Weber, C. Eggeling, H. Grubmuller, S. W. Hell and S. Jakobs, *Proc. Natl. Acad. Sci. U. S. A.*, 2005, **102**, 13070–13074.
93 D. C. Loos, S. Habuchi, C. Flors, J. Hotta, J. Wiedenmann, G. U. Nienhaus and J. Hofkens, *J. Am. Chem. Soc.*, 2006, **128**, 6270–6271.
94 K. Nienhaus, H. Nar, R. Heilker, J. Wiedenmann and G. U. Nienhaus, *J. Am. Chem. Soc.*, 2008, **130**, 12578–12579.
95 G. H. Patterson and J. Lippincott-Schwartz, *Science*, 2002, **297**, 1873–1877.
96 J. N. Henderson, R. Gepshtein, J. R. Heenan, K. Kallio, D. Huppert and S. J. Remington, *J. Am. Chem. Soc.*, 2009, **131**, 4176–4177.
97 J. Lippincott-Schwartz and S. Manley, *Nat. Methods*, 2009, **6**, 21–23.
98 E. Betzig, G. H. Patterson, R. Sougrat, O. W. Lindwasser, S. Olenych, J. S. Bonifacino, M. W. Davidson, J. Lippincott-Schwartz and H. F. Hess, *Science*, 2006, **313**, 1642–1645.
99 M. Fernandez-Suarez and A. Y. Ting, *Nat. Rev. Mol. Cell Biol.*, 2008, **9**, 929–943.
100 J. Lippincott-Schwartz, N. Altan-Bonnet and G. H. Patterson, *Nat. Cell Biol.*, 2003, **Suppl.**, S7–S14.
101 J. Lippincott-Schwartz and G. H. Patterson, *Science*, 2003, **300**, 87–91.
102 J. Lippincott-Schwartz and G. H. Patterson, *Methods Cell Biol.*, 2008, **85**, 45–61.
103 G. H. Patterson and J. Lippincott-Schwartz, *Methods*, 2004, **32**, 445–450.
104 M. Andresen, A. C. Stiel, J. Folling, D. Wenzel, A. Schonle, A. Egner, C. Eggeling, S. W. Hell and S. Jakobs, *Nat. Biotechnol.*, 2008, **26**, 1035–1040.
105 M. Bossi, V. Belov, S. Polyakova and S. W. Hell, *Angew. Chem., Int. Ed.*, 2006, **45**, 7462–7465.
106 M. A. Schwentker, H. Bock, M. Hofmann, S. Jakobs, J. Bewersdorf, C. Eggeling and S. W. Hell, *Microsc. Res. Tech.*, 2007, **70**, 269–280.

 This journal is © The Royal Society of Chemistry 2009